Temperature Response of Isoprene Emission in Vivo Reflects a Combined Effect of Substrate Limitations and Isoprene Synthase Activity: A Kinetic Analysis[1]

Bahtijor Rasulov, Katja Hüve, Irina Bichele, Agu Laisk, and Ülo Niinemets*

Institute of Molecular and Cell Biology, University of Tartu, 510101 Tartu, Estonia (B.R., I.B., A.L.); and Institute of Agricultural and Environmental Sciences, Estonian University of Life Sciences, 51014 Tartu, Estonia (K.H., Ü.N.)

The responses of isoprene emission rate to temperature are characterized by complex time-dependent behaviors that are currently not entirely understood. To gain insight into the temperature dependencies of isoprene emission, we studied steady-state and transient responses of isoprene emission from hybrid aspen (*Populus tremula* × *Populus tremuloides*) leaves using a fast-response gas-exchange system coupled to a proton-transfer reaction mass spectrometer. A method based on postillumination isoprene release after rapid temperature transients was developed to determine the rate constant of isoprene synthase (IspS), the pool size of its substrate dimethylallyldiphosphate (DMADP), and to separate the component processes of the temperature dependence of isoprene emission. Temperature transients indicated that over the temperature range 25°C to 45°C, IspS was thermally stable and operated in the linear range of its substrate DMADP concentration. The in vivo rate constant of IspS obeyed the Arrhenius law, with an activation energy of 42.8 kJ mol^{-1}. In contrast, steady-state isoprene emission had a significantly lower temperature optimum than IspS and higher activation energy. The reversible temperature-dependent decrease in the rate of isoprene emission between 35°C and 44°C was caused by decreases in DMADP concentration, possibly reflecting reduced pools of energetic metabolites generated in photosynthesis, particularly of ATP. Strong control of isoprene temperature responses by the DMADP pool implies that transient temperature responses under fluctuating conditions in the field are driven by initial DMADP pool size as well as temperature-dependent modifications in DMADP pool size during temperature transients. These results have important implications for the development of process-based models of isoprene emission.

Simulation of isoprene emissions from vegetation under fluctuating environmental conditions in the field requires an understanding of how the emissions depend on incident light, ambient and intercellular CO_2 concentrations, and temperature (Guenther et al., 1993, 2006; Wilkinson et al., 2009; Niinemets et al., 2010a, 2010b). So far, the mechanisms responsible for the temperature dependence of isoprene emission are not fully understood, and empirical temperature relationships between isoprene emission and temperature, often considered invariable, are used for modeling the emissions (Guenther et al., 1993, 2006; Niinemets et al., 2010b). However, the temperature responses of isoprene emission do significantly vary among and within species and depending on experimental protocols (e.g. fast versus slow emission response curves; Niinemets et al., 2010b), suggesting that more advanced insight into the temperature dependencies of isoprene emissions are needed to improve the model estimates for ozone formation predictions (Chameides et al., 1988; Fehsenfeld et al., 1992; Paulson et al., 1992). In addition, a mechanistic understanding of the temperature responses of isoprene emissions is needed to evaluate the thermoprotective role of isoprene for the plant photosynthetic machinery (Singsaas et al., 1999; Singsaas and Sharkey, 2000).

Isoprene emission rate at temperatures below 20°C is very low, 5- to 20-fold less than under optimum conditions (Sharkey and Loreto, 1993; Wiberley et al., 2005). At higher temperatures in the steady state, the rate is exponentially increased to the maximum value around 40°C to 42°C (Sanadze and Kalandadze, 1966; Loreto and Sharkey, 1990; Monson et al., 1992; Sharkey and Loreto, 1993; Sharkey et al., 1996; Singsaas and Sharkey, 1998, 2000). Above the maximum, the emission rate decreases to zero at temperatures between 45°C and 50°C (Zimmer et al., 2000). However, under transient conditions, maximum isoprene emissions may be observed even at temperatures as high as 45°C to 50°C (Singsaas et al., 1999; Singsaas and Sharkey, 2000). Both the steady-state and transient emission optima are 10°C to 20°C higher than the optima for photosynthesis (Loreto and Sharkey, 1990; Monson

[1] This work was supported by the Estonian Ministry of Education and Science (grant nos. SF1090065s07 and SF0180045ds08), by the Estonian Science Foundation (grant nos. 7272, 7645, and 8283), and by the Human Frontier Science Programme.

* Corresponding author; e-mail ylo.niinemets@emu.ee.

The author responsible for distribution of materials integral to the findings presented in this article in accordance with the policy described in the Instructions for Authors (www.plantphysiol.org) is: Ülo Niinemets (ylo.niinemets@emu.ee).

www.plantphysiol.org/cgi/doi/10.1104/pp.110.162081

et al., 1992; Guenther et al., 1993; Sharkey and Loreto, 1993; Harley et al., 1997; Singsaas and Sharkey, 2000) and 5°C to 10°C higher than the temperature optimum for photosynthetic electron transport (Niinemets et al., 1999b). This leads to enhanced losses of carbon at supraoptimal temperatures for photosynthesis, approaching 8% to 12% (Sharkey and Loreto, 1993; Sharkey et al., 1996) or even 20% (Harley et al., 1996) of recently formed photosynthates.

The strong temperature dependence of isoprene emission suggests that an enzymatic reaction is the rate-limiting process. In emitting species, isoprene synthase (IspS) catalyzes the final step of the formation of isoprene from dimethylallyldiphosphate (DMADP; Silver and Fall, 1991; Monson et al., 1992; Kuzma and Fall, 1993; Schnitzler et al., 1996; Wildermuth and Fall, 1996; Lehning et al., 1999). Temperature dependence of isoprene emission from leaves was observed to be similar to the temperature dependence of the activity of IspS (Monson et al., 1992). However, the temperature optimum for in vitro IspS was as high as 44.8°C in this study for *Populus tremuloides* (Monson et al., 1992) and even as high as 48°C for *Quercus robur* (Lehning et al., 1999), that is, significantly higher than the optimum temperature for isoprene emissions normally observed in vivo (Sanadze and Kalandadze, 1966; Loreto and Sharkey, 1990; Monson et al., 1992; Sharkey and Loreto, 1993; Sharkey et al., 1996; Singsaas and Sharkey, 1998, 2000). Furthermore, the total IspS activity recovered in vitro has been inadequate to explain the in vivo isoprene emission rates in *Populus trichocarpa* (Wiberley et al., 2008), indicating the necessity to elaborate the in vitro techniques of enzyme isolation and assay.

Another difficulty in directly using the in vitro IspS data to predict the emissions in vivo is that the in vitro enzyme activity measurements are usually made with saturating substrate DMADP concentrations, but the actual chloroplastic DMADP levels responsible for isoprene emission are far below those saturating the enzyme (Brüggemann and Schnitzler, 2002; Loreto et al., 2004; Schnitzler et al., 2005; Rasulov et al., 2009a). This leaves open the possibility that the variation in DMADP concentration may be another important rate-controlling factor of isoprene emission in leaves (Schnitzler et al., 2005; Rasulov et al., 2009b). In fact, some data have indicated significant increases in the 2-*C*-methyl-D-erythritol 4-phosphate (MEP) pathway activity and DMADP concentration when the rate of isoprene emission increased at elevated temperature (Wolfertz et al., 2003; Magel et al., 2006).

Finally, IspS activity may change temporarily due to slow transcriptional and posttranscriptional processes (Mayrhofer et al., 2005; Sasaki et al., 2005; Wiberley et al., 2005) via the modulation of the promoter (Cinege et al., 2009) or via faster allosterically controlled enzyme activation processes (Singsaas and Sharkey, 1998). For example, regulation of expression of IspS and MEP pathway enzyme genes in *P. trichocarpa* can be initiated within minutes to hours in response to a temperature signal.

This evidence collectively indicates that several processes can play a role in determining the shape of the temperature dependence of isoprene emission. The possible processes from fastest to slowest response time are as follows: (1) the direct effect of temperature on the kinetic rate constant of IspS at a constant amount of the active enzyme and a constant substrate concentration; (2) the concentration of the substrate DMADP may change due to the readjustments of the balance between the intermediates of the MEP pathway; (3) the amount of the active IspS enzyme molecules may vary due to the temperature-dependent efficiency of an allosteric activator, if such an activator exists; and (4) the total amount of the enzyme protein may vary due to the temperature-dependent balance of protein synthesis and degradation. In this work, we have made use of the fast response time of processes 1, 2, and 3 to gain insight into their role in the regulation of the temperature-dependent isoprene emission from leaves. All experiments were conducted with hybrid aspen (*Populus tremula* × *Populus tremuloides*) that is a strong isoprene emitter (Rasulov et al., 2009a, 2009b).

RESULTS

Photosynthetic Temperature Dependencies in Steady State

In the steady-state experiments conducted at an ambient CO_2 concentration of 380 μmol mol^{-1}, the optimum temperature for net CO_2 uptake (Eq. 3) was 25.9°C (Fig. 1A). Low optimum temperature for net assimilation was partly associated with increasing respiration and photorespiration with increasing temperature (Fig. 1A), as the optimum temperatures for photosynthetic electron transport, whether determined from chlorophyll fluorescence (Eq. 1) or from gas exchange (Eq. 2), were larger, 30.9°C to 31.5°C (Fig. 1B). Both the estimates of photosynthetic electron transport from fluorescence (J_F; Eq. 1) and gas exchange (J_G; Eq. 2) were strongly correlated throughout the temperature response.

During the measurements, stomata tended to close at higher temperatures despite keeping water vapor pressure constant (Fig. 1C). However, since the CO_2 exchange rate decreased, the intercellular CO_2 concentration changed little over the temperature range 25°C to 35°C and actually increased at higher temperatures, indicating that leaf photosynthetic activity decreased more than stomatal conductance at these high temperatures.

Interaction of Steady-State Isoprene Temperature Responses with CO_2 Concentration

Isoprene emission rate had a maximum at 39°C (Fig. 2) that is significantly higher than that either for the net assimilation rate (Fig. 1A) or for the photosynthetic electron transport rate (Fig. 1B). Given the changes in intercellular CO_2 concentrations with temperature

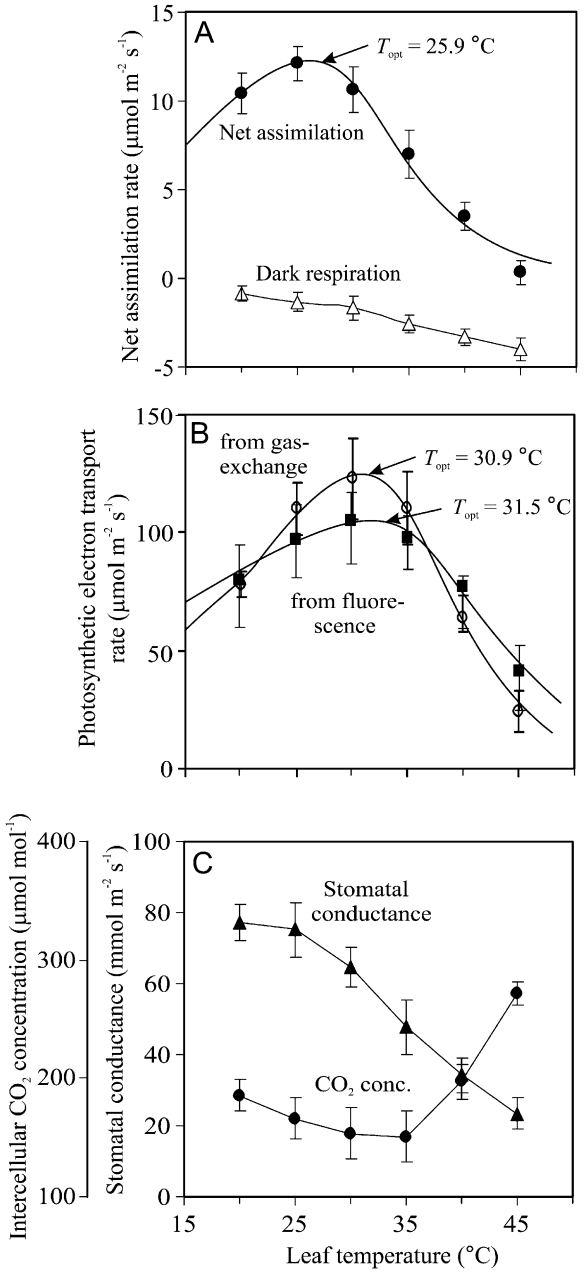

Figure 1. Steady-state temperature dependencies of net CO_2 assimilation and dark respiration rates (A), photosynthetic electron transport rate from chlorophyll fluorescence (Eq. 1) and from gas exchange (Eq. 2; B), and stomatal conductance to water vapor and intercellular CO_2 concentration (C) in hybrid aspen leaves at ambient CO_2 concentration of 380 μmol mol^{-1} and oxygen concentration of 210 mmol mol^{-1}. Data for the net assimilation rate (A) and photosynthetic electron transport (B) were fitted by Equation 3, and the optimum temperatures (T_{opt}) were calculated by Equation 4. Error bars show SD of five replicate experiments.

(Fig. 1C), the question is whether the temperature dependence of isoprene emission may be partly driven by CO_2 effects. We observed an inhibition of isoprene emissions by high CO_2 at lower temperatures (Fig. 3). For example, at 22°C, isoprene emission rate decreased by about 50% when CO_2 concentration was increased from 390 to 800 μmol mol^{-1}. However, the inhibitory effect of CO_2 gradually decreased with increasing temperature, and at 40°C there was no statistically significant effect of CO_2 on isoprene emission (Fig. 3). Given the temperature responses of isoprene emission (Fig. 2), intercellular CO_2 concentration (Fig. 1C), and the temperature sensitivity of CO_2 inhibition of isoprene emission (Fig. 3), we conclude that the modifications in intercellular CO_2 concentration (Fig. 1C) did not dominate the temperature response of isoprene emission.

Temperature Dependencies of Isoprene Emission and the DMADP Pool in the Steady State

Postillumination measurements were carried out at different temperatures in the steady state, and the DMADP pool sizes corresponding to the given temperature were obtained (Fig. 2). Characteristically, the DMADP pool size had a maximum value at 35°C (Fig. 2), that is, at somewhat higher temperature than the rate of photosynthetic electron transport (Fig. 1B) and lower than for isoprene emission rate. The activation energy for isoprene emission in steady-state conditions was 72.1 kJ mol^{-1} and that for DMADP pool size was 56.6 kJ mol^{-1}, indicating greater enhancement of isoprene emissions with increasing temperature than can be predicted from changes in DAMDP pool size alone. Thus, these data suggest that up to 35°C, the enhancement of isoprene emissions is associated with both the increase of the substrate pool size and the acceleration of the IspS reaction. At temperatures beyond 35°C, the steady-state DMADP pool size de-

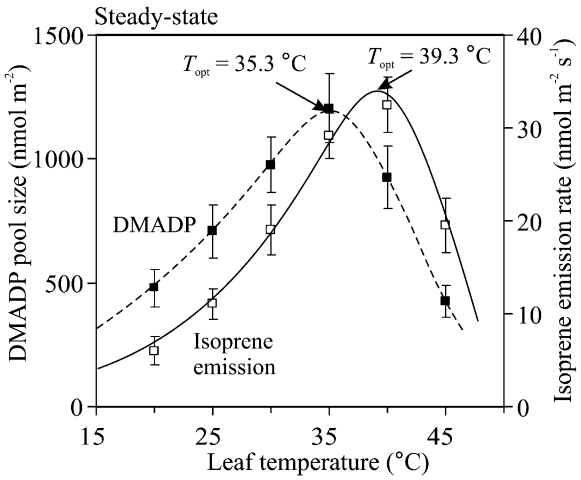

Figure 2. Comparison of the temperature dependencies of steady-state isoprene emission rate and the corresponding DMADP pool size. DMADP pool size was measured as the integral of postillumination isoprene emission after light was turned off in the steady state (see "Materials and Methods"). Error bars correspond to SD of four to 10 replicate experiments. Data were fitted by Equation 3, and the optimum temperatures (T_{opt}) were calculated by Equation 4.

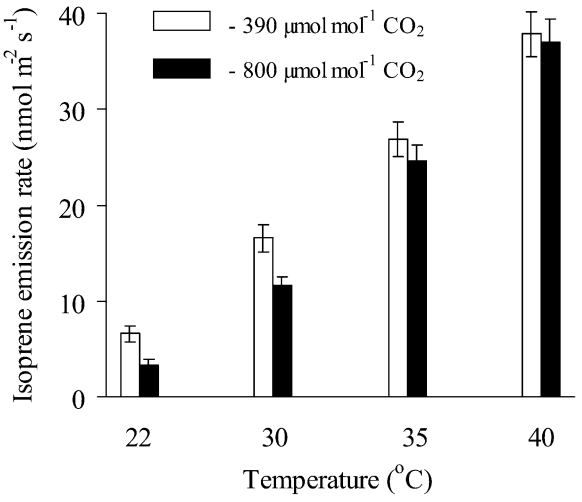

Figure 3. Comparisons of steady-state isoprene emission temperature dependencies at current ambient CO_2 concentration of 390 μmol mol^{-1} and at high CO_2 concentration of 800 μmol mol^{-1}. Error bars give SD of five replicate experiments. The isoprene emission rate is significantly larger under ambient than under high CO_2 at 22°C and 30°C, but no significant CO_2 effect is observed at 35°C and 40°C ($P > 0.05$, ANOVA).

creases, but the direct effect of temperature on the enzyme activity is stronger than the reduction of substrate availability. Thus, isoprene emission rate continues to increase with temperature, although with a slower rate. However, between 40°C and 45°C, both the DMADP pool size and isoprene emission rate decrease (Fig. 2). Whether this reduction in the emission rate results from a decrease in the enzyme activity at supraoptimal temperature or from a reduced DMADP pool size cannot be resolved from such steady-state experiments. With the following dynamic experiments, we tried to determine the true temperature response of the IspS reaction free of the simultaneous variations in the DMADP pool size.

Transient Changes in Isoprene Emission Rate after Temperature Changes

Experiments with rapid temperature responses revealed reproducible multiphasic temperature responses of isoprene emission (Fig. 4). Changing the temperature from 33°C to 25°C produced a two-phase transient, where the fast initial decrease in the emission rate was followed by a slow phase lasting about 2 to 3 min. The reversal to 33°C exhibited a similar transient character. However, transient responses at high temperatures were more complex. As with lower temperature, the initial fast increase was followed by a slower increase. However, the increasing phase was replaced by a time-dependent reduction of the emission rate a few minutes after reaching the maximum at 40°C and 44°C, while the emissions started to virtually decline immediately after reaching the peak value at 50°C (Fig. 4). Already the temperature of 44°C was close to the threshold for leaf damage; it took about 30 min to recover to the initial rate at 33°C (Fig. 4). The highest applied temperature of 50°C was lethal during prolonged exposures.

Temperature Dependencies of the Rate Constant of IspS and Isoprene Emission at Constant DMADP

What is causing the multiphasic temperature response of isoprene emissions in Figure 4? The isoprene emission rate determined from the temperature/light transients and at a constant DMADP pool size corresponding to 33°C had an optimum temperature of 47.6°C (Fig. 5). In addition, the slope of the DMADP versus isoprene emission rate relationship (Fig. 6), the rate constant of IspS, increased from 0.013 ± 0.002 s^{-1} (average ± SD) at 25°C to 0.039 ± 0.003 s^{-1} at 50°C with the apparent temperature optimum of 48.3°C (Fig. 5). From these measurements, the activation energy (Eq. 5) obtained for the IspS was 42.8 kJ mol^{-1}, while the activation energy was 47.0 kJ mol^{-1} for isoprene emissions at a constant DMADP pool.

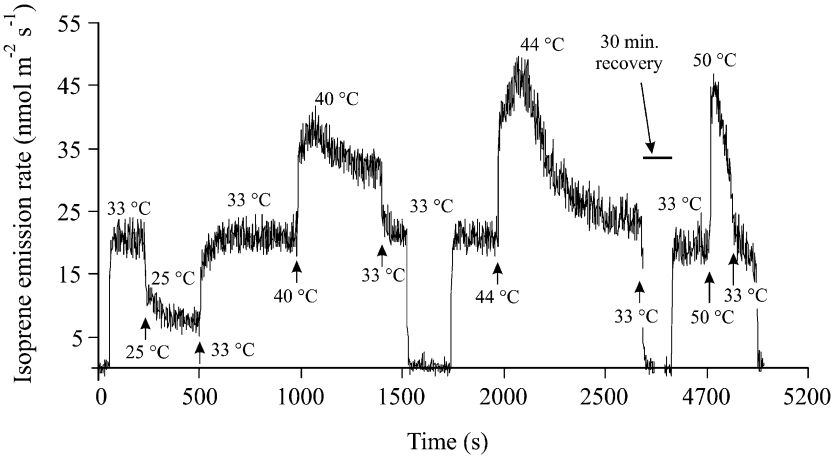

Figure 4. Original PTR-MS recording of transients in isoprene emission following rapid changes in temperature. The leaf was always stabilized at 33°C, and temperature was changed step-wise down and up from this reference value. After the exposure to 44°C, the recovery at 33°C required an additional 30 min. In the figure, during the periods with zero isoprene emission, the system was changed to the reference stream. Four replicate experiments were conducted, and in each case reproducible kinetics were observed.

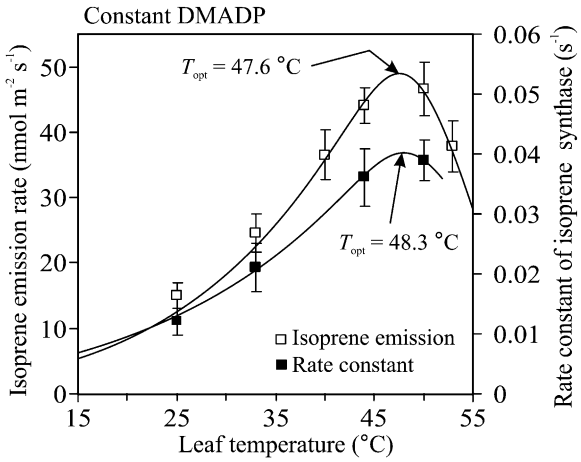

Figure 5. Comparison of the temperature dependencies of the isoprene emission rate and the rate constant of the IspS at a constant DMADP pool size based on the dynamic experiments. In these experiments, the DMADP pool size corresponds to the steady-state isoprene emission rate at 33°C (the experiments with simultaneous darkening and change in leaf temperature; see "Materials and Methods"). The rate constant was calculated as the slope of isoprene emission rate versus DMADP pool size during the dark isoprene emission transients (see "Materials and Methods"). Error bars denote SD of four to nine replicate experiments at each temperature. Data fitting as in Figure 2.

Is There Evidence of Temperature-Dependent Variation in the Activation State of IspS?

To study the possibility of enzyme activation in the complicated transients (increase of emissions during 0–150 s after an increase of temperature from 33°C to 40°C to 45°C in Fig. 4), the kinetic constant of IspS was first measured immediately after the temperature change from 33°C to 44°C (Fig. 6A), and then the experiment was repeated measuring the kinetic curve 120 s after the change (Fig. 6B), at the time when the isoprene emission rate was the fastest (Fig. 4). These experiments showed no change ($P > 0.05$) in the rate constant of IspS (Fig. 6C), but the DMADP pool size was approximately 20% larger when the emission rate was faster. Analogous experiments with longer waiting times indicated that the final slow rate of isoprene emission established in the steady state at high temperatures (Fig. 2) was accompanied by a drastic decrease in the DMADP pool size (data not shown).

Additional experiments were conducted by using different initial DMADP pool sizes either due to different initial temperature (Fig. 7A) or different light intensity (Fig. 7B). These experiments indicated that the leaves with a higher initial DMADP pool (higher initial temperature or higher light) had greater initial isoprene emission rates after the transfer of the leaves to higher temperature (Fig. 7). In these experiments, an average (±SD) 92% ± 37% increase in DMADP pool size by manipulations of initial temperature or light was associated with a 58% ± 11% increase in initial isoprene emission rate after the change in temperature. However, further increase of the emissions within the following 120 s was greater in leaves with a lower initial DMADP pool, indicating that isoprene emission was more strongly limited by DMADP pool size in leaves with lower initial DMADP pool size. These experiments collectively suggest that the activation state of IspS did not change during the investigated transients of about 10 min.

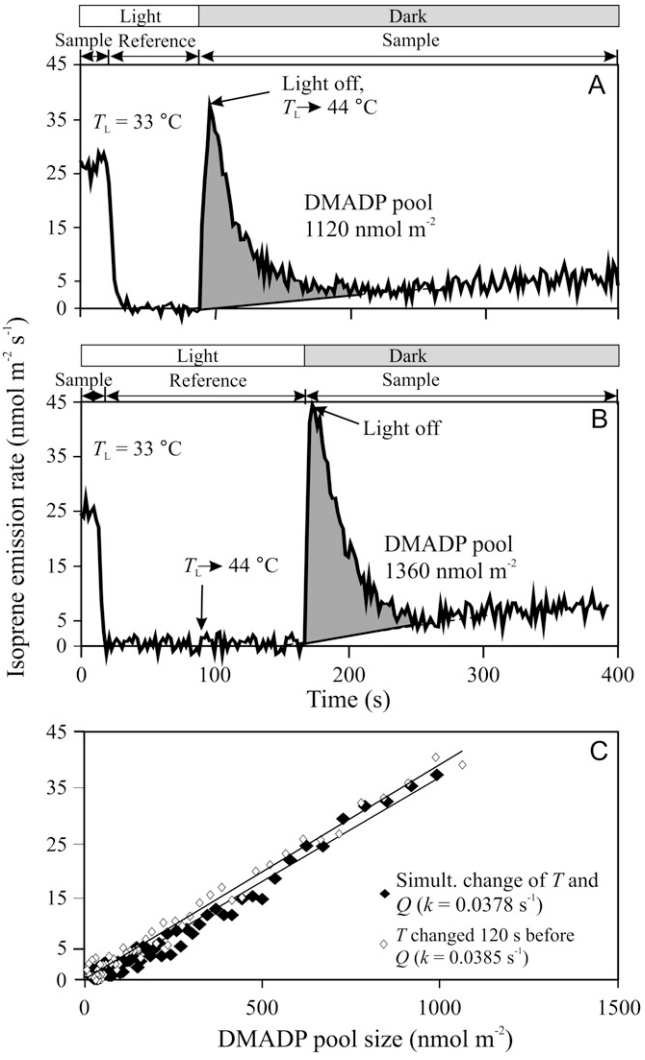

Figure 6. Sample responses of the kinetics of dark isoprene emission following temperature changes (A and B) and corresponding isoprene emission versus DMADP pool size relationships (C). In A, temperature was increased from 33°C to 44°C and light (Q) was switched off simultaneously, while in B, temperature was raised 120 s before switching off the light. The shaded areas in A and B correspond to the total DMADP pool size responsible for isoprene emission in light. The dark decay kinetics was employed to obtain the paired values of the isoprene emission rate and DMADP pool size (see "Materials and Methods"). The slope of the linear regression fitted to isoprene emission rate versus DMADP pool size relationship provides the first-order rate constant of IspS reaction (k; s^{-1}). Isoprene evolution versus DMADP pool size relationships suggest that IspS activity did not change during this 120-s delay period (similar k values).

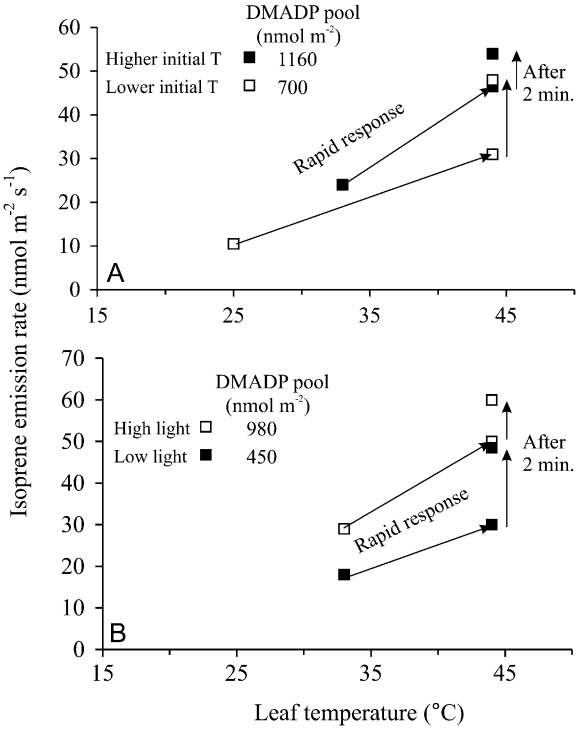

Figure 7. Representative illustrations of the effect of the initial DMADP concentration on the rapid temperature response kinetics of isoprene emission. Initial DMADP concentration was either changed by altering the initial temperature in the steady state (A; 25°C versus 33°C) or by changing the incident quantum flux density (B; 300 versus 600 μmol m^{-2} s^{-1}), and the emission rates were determined at different times during the temperature transients (for transient temperature responses of emissions, see Fig. 4).

DISCUSSION

Steady-State Temperature Responses of Photosynthetic Processes and Isoprene Emission

Both the temperature dependencies of isoprene emission and photosynthetic CO_2 uptake have a maximum, followed by a range where increasing temperature is accompanied by a decreasing rate of the process (Figs. 1 and 2). Such a temperature response is difficult to explain thermodynamically, except when the biological machinery of the process is being destroyed by the high temperature. This evidently happens at temperatures above 45°C to 50°C, where the response becomes irreversible (Hüve et al., 2010). However, there is a range of temperatures between 40°C and 45°C for isoprene emission and between 30°C and 45°C for photosynthetic CO_2 uptake, where the inhibition of the process is rapidly reversible when the leaves are returned to lower temperature (Fig. 1A). The high-temperature inhibition of net CO_2 uptake is partly explained by increasing photorespiratory and mitochondrial CO_2 evolution; however, photosynthetic electron transport is inhibited at high temperature as well (Fig. 1B). In this work, we specifically investigated the causes of the reversible inhibition of isoprene emission; at temperatures exceeding the heat stress tolerance limit, the causes for inhibition may be similar for both processes.

Kinetic Approach for Understanding the Temperature Responses of Isoprene Emission

As outlined in the introduction, the in vivo temperature dependence of isoprene emission can result from a variety of component processes with different time kinetics. Out of these, changes in the total amount of the IspS protein as the result of temperature-dependent shifts in the rates of protein synthesis and degradation typically have half-times on the order of hours (Loivamäki et al., 2007; Wiberley et al., 2009) and, therefore, are unlikely to play a role in the dynamics discussed here. To separate between various shorter term processes potentially affecting the temperature responses of isoprene emissions, such as changes in the IspS kinetics at constant substrate concentration and enzyme activation state, modifications in the substrate concentration, and adjustments in the enzyme activation state, a kinetic method was developed based on transient temperature responses of isoprene emission. Fast temperature changes were achieved by alternating between the thermostats feeding the water jacket of the leaf chamber. This way, rapid exponential changes in leaf temperature with a time constant of 3 s (6–10 s for full stabilization; Fig. 8) were achieved. Such temperature jumps induced complex transients of isoprene emission composed of an almost immediate initial response, followed by further monotonous or dual-phase adjustment with the characteristic time constants of about 100 s and 300 to 400 s (Fig. 4). Furthermore, the transient responses were

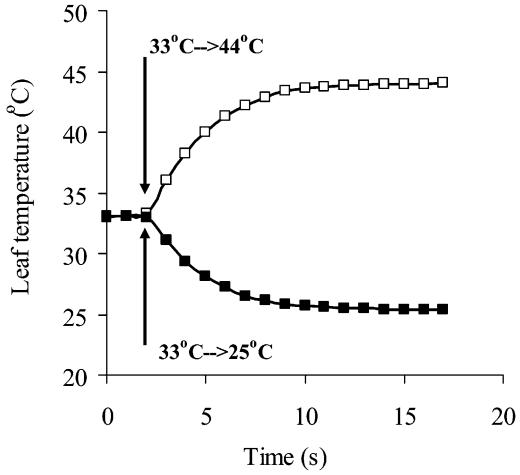

Figure 8. Demonstration of the inherent temperature response of the measurement system during the rise (white squares) and decrease (black squares) of temperature. The temperature of the leaf chamber water jacket was controlled by two precision thermostats set at different temperatures. At time 2 s, either the thermostat with higher (white squares) or lower (black squares) temperature was switched to the leaf chamber water jacket.

combined with an analysis of postillumination isoprene transients to determine the DMADP pool sizes (Figs. 6 and 9) and determine the rate constant of isoprene emission (Figs. 6 and 10). After the temperature was changed, light was turned off and the postillumination decay of isoprene emission was measured at a new temperature, but with the substrate pool accumulated at the preceding temperature. Previously, we have used this technique for investigation of the kinetics of Rubisco at various temperatures (Oja et al., 1988) and of IspS kinetics at a constant temperature (Rasulov et al., 2009a). Here, this technique was applied for the measurement of the kinetic rate constant of IspS at different temperatures with a constant substrate DMADP pool size (Figs. 5 and 10).

Temperature Dependence of IspS Activity in Vivo

Although the fastest component process is likely determined by the kinetic response of enzyme chemistry (Singsaas and Sharkey, 1998), in previous temperature experiments the IspS kinetics could not be separated from changes in substrate concentration. In our study, the analysis of the temperature transients combined with DMADP pool size estimations showed that, in vivo, IspS reaction is operating in the first-order kinetic range, with the maximum (average ± SD) rate constant of 0.0401 ± 0.003 s^{-1} predicted to occur at the optimum temperature of 48.3°C (Figs. 5 and 10). Over the temperature range 25°C to 44°C, the temperature response of the rate constant of IspS exhibited a strictly exponential increase, with the Arrhenius activation energy of 42.8 kJ mol^{-1} (Fig. 5) indicating that the IspS enzyme is thermodynamically stable and follows the Arrhenius response at least to temperatures as high as 45°C to 48°C. This is in accordance with in vitro studies showing the optimum of IspS activity between 45°C and 50°C (Monson et al., 1992; Lehning et al., 1999), although in some cases lower temperature optima have been observed (Schnitzler et al., 2005).

Substrate Limitations as Responsible for the Reduction of Isoprene Emissions below the Temperature Optimum for IspS

The observed first-order IspS kinetics imply that a decreasing DMADP pool size is a potential cause for the reduction of the steady-state rates of isoprene emissions at temperatures below the threshold for thermal damage. Our results (Fig. 2) confirmed this hypothesis, showing that the steady-state DMADP pool size reaches the maximum at 35.3°C. The maximum of isoprene emission is shifted toward higher temperature with an optimum at 39.3°C (Fig. 2). Thus, the decrease in the DMADP pool size is more than compensated by the increasing rate constant of IspS (Fig. 5). On the other hand, simultaneous increases of DMADP pool size and IspS rate constant resulted in high activation energy for isoprene emission of 72.1 kJ mol^{-1} over the temperature range of 20°C to 35°C. Analogously

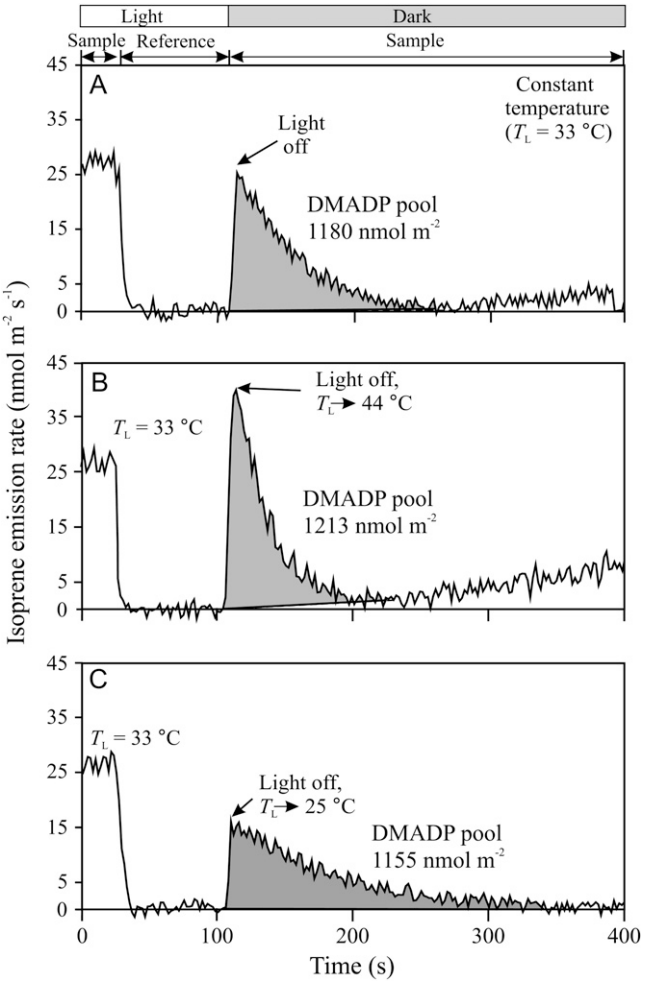

Figure 9. Original PTR-MS recordings of the measurements of the transient responses of isoprene emissions of hybrid aspen leaves after switching off the light either under constant leaf temperature (A) or after simultaneously changing leaf temperature and switching off the light (B and C). The postillumination transients were used to determine the size of the DMADP pool responsible for isoprene emission according to the method of Rasulov et al. (2009a, 2009b). An ultrafast gas-exchange system with a response time of approximately 3 s was used (Laisk et al., 2002). The recording begins in a steady state at leaf temperature (T_L) of 33°C (0–40 s), then the reference line of the mass spectrometer is recorded between 40 and 100 s, followed again by the leaf sample. In A, light was switched off at 106 s and dark evolution of isoprene was followed until reaching the baseline. In B, the leaf chamber water jacket was switched to the thermostat with T_L = 44°C, and in C, it was switched to T_L = 25°C, at 100 s, and 6 s later, the leaf chamber was switched from channel 1 to channel 2 and the light was turned off simultaneously. The delay of 6 s was used to account for the slightly slower response of temperature change (Fig. 8) than the response of the gas-exchange part of the system. The integral of isoprene emission provides the DMADP pool size responsible for isoprene emission (Rasulov et al., 2009a, 2009b). As at higher temperatures, a slower component of isoprene dark emission was also observed; the baseline for integration in B was adjusted to consider this component (dashed line), as explained in "Materials and Methods." In these experiments, ambient CO_2 concentration was 380 μmol mol^{-1} and O_2 concentration was 210 mmol mol^{-1}. Average ± SD DMADP pool sizes and isoprene emission rates corresponding to replicate experiments are demonstrated in Figures 2 and 5.

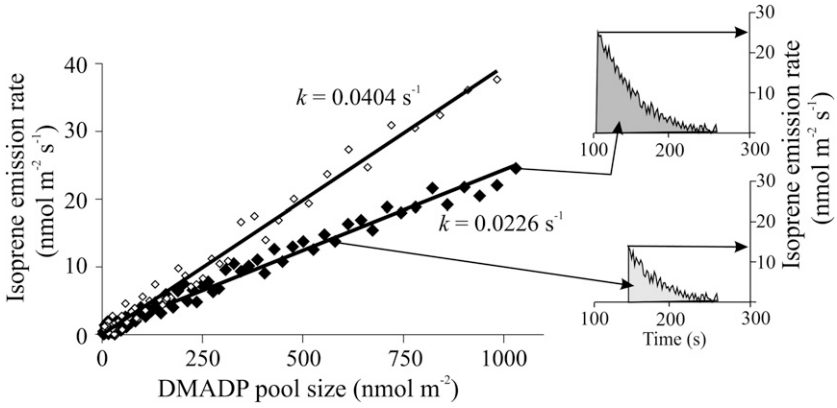

Figure 10. Determination of the rate constant of the IspS reaction based on the transients shown in Figure 9. The total DMADP pool size is the integral from the time of darkening (t_0) to reaching the baseline level (t_f). This DMADP pool size corresponds to the isoprene emission rate at the time of darkening (top inset for the data from Fig. 9A). Integrating backward from time t_f to arbitrary time t provides a DMADP pool size that corresponds to the isoprene emission rate at this time t (bottom inset). Thus, for any isoprene emission rate in the dark, we obtained the corresponding pool sizes. For a first-order reaction, a linear dependence is expected between the pool size and the IspS reaction rate. Accordingly, the slope of this dependence provides the rate constant of the IspS reaction. The black symbols correspond to the dark measurements at 33°C (Fig. 9A), while the white symbols correspond to the measurements at 44°C (Fig. 9B). Average isoprene emission rates and rate constants derived from replicate experiments are shown in Figure 5.

high activation energies of isoprene emission even up to 100 kJ mol^{-1} have been observed in other studies as well (Harley et al., 1996; Hanson and Sharkey, 2001).

The importance of variations in the DMADP pool size in temperature-dependent changes in isoprene emissions above 30°C has been emphasized before (Magel et al., 2006; Nogués et al., 2006). In fact, a general negative relationship between isoprene emission and its substrate pool was suggested (Nogués et al., 2006). However, as shown by Singsaas and Sharkey (2000), Magel et al. (2006), and our study, such a reciprocity is observed only over a narrow temperature range above 35°C, where the exponential temperature response of IspS kinetics overruns the effect of the decreasing DMADP pool.

Dynamic Variation in DMADP Pool Size in Temperature Transients

In the transient temperature experiments, after temperature is rapidly increased to temperatures of 40°C to 44°C, the DMADP pool first increases during about 200 s and then decreases during about 10 min (Fig. 4). Given the thermal stability of IspS over this temperature range, and the rapid reversibility of the transient response, we conclude that the slow decrease in the isoprene emission rate, in approximately 200 s after the change of the temperature from 33°C to 40°C (Fig. 4), is caused by slowly decreasing pool of DMADP. However, what is the cause for the initial increase of the emissions in the transient lasting for about 200 s (Figs. 4, 6, and 7)? Can this enhancement reflect an increase of the activation state of the IspS enzyme on the background of the decreasing DMADP pool? In fact, the results in Figures 6 and 7 suggested that the pool size of DMADP was increasing during the initial period of increasing isoprene emission, while the rate constant of IspS did not change (Fig. 6). This result does not support the suggested variation of IspS activation state with temperature (Monson et al., 1992; Singsaas and Sharkey, 1998).

To explain the initial enhancement of DMADP pool size after the temperature increase, DMADP synthesis immediately after the transient must increase even faster than the rate of isoprene synthesis from DMADP. Overall, such complex transient responses to increasing temperature suggest that different reactions in the MEP pathway of DMADP synthesis respond differently to the increasing temperature. We hypothesize that the initial enhancement of DMADP synthesis is related to enhancement of the terminal reactions of the MEP pathway, that is, those beginning with 2-phospho-4-(cytidine 5-diphospho)-2-*C*-methyl-D-erythritol (Fellermeier et al., 2001; Rohdich et al., 2001). However, the reactions coupled with energetic cofactors ATP and CTP soon slow down, probably because of the decreasing ATP level at elevated temperatures. As soon as the pools of 2-phospho-4-(cytidine 5-diphospho)-2-*C*-methyl-D-erythritol and 2-*C*-methyl-D-erythritol 2,4-cyclodiphosphate are exhausted, the rate of the whole pathway slows down to the rate determined by the availability of ATP and CTP.

ATP as Ultimately Limiting the Formation of DMADP Synthesis?

There are two basic hypotheses about the rate limitation of the whole MEP pathway of isoprene synthesis. The concept of regulation by the input of carbon moieties (Rosenstiel et al., 2003) assumes the rate-

limiting role of the availability of mainly phospho*enol*-pyruvate (and pyruvate) and glyceraldehyde-3-phosphate, the compounds condensing to form 1-deoxy-D-xylulose 5-phosphate (Lichtenthaler, 1998). These same substances are feeding carbon to the Krebs cycle of mitochondrial respiration. The increasing rate of dark respiration at elevated temperatures may outcompete the MEP pathway for the input carbon, limiting the rate of isoprene emission. However, such a competition is more efficient in rapidly respiring young leaves but not in mature leaves showing fast rates of the MEP pathway and reduced rates of respiration (Centritto et al., 2005). Our results (Figs. 1 and 2) showed rather parallel courses of respiration and isoprene emission rates along different temperatures, in accord with Loreto et al. (2007) and Fortunati et al. (2008) and not consistent with the competition between these two processes, at least in the range of temperatures below 45°C. The insensitivity of isoprene emissions to CO_2 under higher temperature (Fig. 3; Affek, 2003) is also in line with the conclusion that carbon input is not limiting the rate of the MEP pathway. In several studies under moderate temperatures of approximately 30°C, it has further been reported that the photosynthetically generated carbon pools are sufficient to support normal isoprene emission rates for extended periods of time (Sharkey and Loreto, 1993; Pegoraro et al., 2004) as soon as the CO_2 uptake rate exceeds the CO_2 compensation point (Tingey et al., 1981; Wolfertz et al., 2003; Rasulov et al., 2009b). In fact, this condition does not change in high-temperature stress (Darbah et al., 2010).

Alternatively, variations in the DMADP pool size in response to these environmental parameters have been associated with variations in the levels of energetic metabolites, in particular ATP, generated in photosynthesis (Rasulov et al., 2009b). As discussed above, sustained time-dependent inhibition of DMADP pool size after transfer to higher temperatures is consistent with a reduction in the pool size of ATP- and CTP-dependent intermediates. So far, there is not much information about chloroplastic ATP levels being dependent on temperature. However, indirect evidence is consistent with temperature-dependent reductions in chloroplastic ATP. The rate of photosynthetic electron transport decreases at higher temperatures (Niinemets et al., 1999b; Fig. 1B), suggesting the possibility that at moderately high temperatures, the efficiency of the photosynthetic machinery to generate energetic metabolites reversibly decreases. Moderate heat stress increased the proton conductance of thylakoid membranes in a time-dependent manner in Arabidopsis (*Arabidopsis thaliana*) leaves (Zhang and Sharkey, 2009) and reduced the pH component of the transthylakoid proton motive force in tobacco (*Nicotiana tabacum*) leaves (Zhang et al., 2009). Probably the most convincing evidence comes from measurements in isolated chloroplasts and thylakoids, where the coupling of the photosynthetic electron flow with proton transport and ATP synthesis was more sensitive to moderately high temperature than the uncoupled electron transport to methyl viologen. The coupling ratio, ATP/$2e^-$, decreased continuously with temperature above 35°C, indicating temperature-induced uncoupling and/or proton leak (Stidham et al., 1982). In the latter study, the optimum of ATP synthesis was found at 30°C to 33°C (Stidham et al., 1982), being very close to the temperature optimum of DMADP in our experiments (Fig. 2).

Although variation in the chloroplastic ATP levels is a good candidate to explain the reversible reduction of DMADP pool size under moderately high temperatures, further efforts are needed to understand the reasons suppressing ATP synthesis under these and other stress conditions. Temperature-dependent modifications in the importance of the proton-uncoupled cyclic electron flow around PSI can provide an explanation for the reversible reduction of ATP levels (Laisk et al., 2010). At elevated temperatures, the glycolytic direction of the Calvin-Benson cycle may dominate over the photosynthetic direction. As a result, the pressure of NADPH and associated reduced ferredoxin may increase to the extent that electrons from ferredoxin via the cyclic pathway to the donor side saturate the transport capacity of PSI, partly outcompeting the linear electron flow.

CONCLUSION

These data suggest that the steady-state temperature response of isoprene emission results from changes in isoprene precursor, DMADP, pool size, and from modifications in the rate constant of IspS. Due to inherently different temperature responses of IspS and other MEP pathway reactions supplying DMADP, the temperature responses of isoprene emission are different under transient and steady-state conditions. Constancy of IspS under transient conditions implies that the initial conditions that determine DMADP pool size can importantly modify the emission responses to fluctuating temperature conditions in the field. Depending on the previous leaf temperature and light environment, the leaf isoprene emission response to a heat pulse is different (Fig. 7). These results collectively have important implications for understanding the isoprene emission fluctuations in field environments and make it possible to more effectively link the isoprene emission models to kinetics of IspS. Overall, the MEP pathway and isoprene emission in chloroplasts seem to be tightly linked to photosynthesis via common energetic substrates. However, additional work is clearly needed to gain insight into the biochemical determinants of the DMADP synthesis rate under different temperatures.

MATERIALS AND METHODS

Plants and Growth Conditions

One-year-old plants of hybrid aspen (*Populus tremula* × *Populus tremuloides* clone 200; for the genotype, see Vahala et al., 2003) were grown in an AR-95

HIL climatic chamber (Percival CLF Plant Climatics) in 4-L plastic pots filled with a mixture of peat and sand (1:1) at optimized water and nutrient supply, as described by Rasulov et al. (2009a, 2009b). Quantum flux density of 550 μmol m^{-2} s^{-1} was provided during a 14-h photoperiod, day/night temperatures were 26°C/20°C, and relative humidity was kept at 60% ± 2%. Preliminary experiments demonstrated that under such growth conditions, isoprene emission starts 5 to 6 d after leaf emergence. Thus, only fully developed leaves 20 to 30 d after bud burst were used in all experiments.

Transient and Steady-State Measurements of CO_2 and Water Vapor Exchange

A fast two-channel gas-exchange system was used for the measurements (Laisk et al., 2002). The attached leaf was enclosed in a clip-on-type leaf chamber (8.04 cm^2 cross-section area and 0.3 cm height). The flow rate of the system was maintained at 0.5 mmol s^{-1} (Laisk and Oja, 1998). Given the volume of the leaf chamber of only 2.4 cm^3, and assuming first-order kinetics, the leaf chamber half-time was 0.15 s (for calculation of chamber time response, see Li-Cor, 2001; Weiss et al., 2009). Thus, the chamber effect on the kinetic patterns studied can be considered negligible.

While the leaf chamber was connected to channel 1, the water vapor, CO_2, and isoprene analyzers recorded the reference lines at channel 2. As soon as the chamber was connected to channel 2 (in less than 1 s), the analyzers immediately recorded the corresponding gas-exchange rates with a minor, 1- to 2-s delay (Laisk et al., 2002). Thus, this setup is particularly advantageous for fast measurements, avoiding the time delays resulting from analyzer matching for two analyzer systems and delays due to stabilization of gas flows in single analyzer systems with nonequivalent resistances of different channels.

Synthetic air for both channels was mixed from pure nitrogen, oxygen, and CO_2 with dynamic mixers. The CO_2 concentration was measured with an infrared CO_2 analyzer (LI-6251; Li-Cor), while the water vapor pressure was measured with a psychrometer integrated in the gas system (Laisk et al., 2002). For the high-temperature measurements, the whole gas system, including tubing and psychrometers, was thermostatted at 50°C.

To enhance the temperature exchange, the upper leaf surface was glued with starch paste to the thermostatted glass window of the leaf chamber water jacket. This did not block foliar gas exchange, because aspen has essentially no stomata on the upper leaf side. Less than 2% of isoprene emission occurs through the upper epidermis of aspen leaves (Fall and Monson, 1992). The advantage of gluing the leaf on the window of the gas-exchange chamber is that the leaf heat-exchange coefficient is increased by about ten times. Thus, leaf temperature is stabilized practically independently of incident light intensity and leaf evaporation rate. Leaf chamber temperature was controlled at the desired temperature by two thermostats as described by Niinemets et al. (1999a). The two-thermostat system with a four-way custom-made valve was constructed to allow for rapid leaf temperature transients. One thermostat was circulating the water through the leaf chamber water jacket, while in the second thermostat the next temperature was established. By switching between the thermostats, fast step-wise changes in leaf temperature could be induced. The rate of change of the leaf temperature obtained this way had a half-time of approximately 3 s (i.e. the new temperature was established in approximately 10 s; Fig. 8). Although the temperature change was slower than the response time of the gas-exchange measurements by this system, such temperature jumps still allowed us to distinguish between the partial rate-limiting reactions of isoprene emission. The humidity of the inlet gas was increased in parallel with the increasing leaf temperature such that it remained constant during the measurements of the temperature response curves.

Standard conditions used in these experiments were as follows: leaf temperature of 33°C, saturating incident quantum flux density of 600 μmol m^{-2} s^{-1} (Schott KL 1500 halogen light source), ambient CO_2 concentration of 380 μmol mol^{-1}, oxygen concentration of 210 mmol mol^{-1}, and inlet gas water vapor pressure deficit of 1.7 kPa. After enclosure of the leaf in the chamber, the standard environmental conditions were established and the leaf was maintained at these conditions until stomata opened and steady-state CO_2 and isoprene emission rates were established, typically 15 to 20 min after leaf enclosure. Thereafter, leaf temperatures were step-wise changed to record either the steady-state values at each temperature and/or the transient responses with constant and varying DMADP pool size (see below).

Foliage gas-exchange rates, stomatal conductance, and intercellular CO_2 concentration were calculated using standard procedures (von Caemmerer and Farquhar, 1981).

Determination of the Rate of Photosynthetic Electron Transport

Chlorophyll fluorescence was measured concurrently with foliage gas exchange by a PAM 101 fluorimeter (H. Walz). Saturated pulses of white light of 14,000 μmol m^{-2} s^{-1} for 2 s provided by the second Schott KL 1500 light source were given to measure the maximum fluorescence yield of light-adapted samples (F_m'). The quantum yield of PSII electron transport in light (Φ_{PSII}) was calculated as $(F_m' - F)/F_m'$, where F is the steady-state fluorescence yield. The rate of photosynthetic electron transport from chlorophyll fluorescence (J_F) was further calculated as (Schreiber et al., 1994):

$$J_F = f_{PSII}\alpha\Phi_{PSII} \quad (1)$$

where f_{PSII} is the fraction of light absorbed by PSII (taken as 0.5 in this study) and α is the leaf absorptance (taken as 0.89 in this study; Niinemets et al., 1999a). In addition, the electron transport rate needed to explain the observed gas-exchange rates (J_G) was also calculated from the net assimilation rate (A), dark respiration rate (R_d), and intercellular CO_2 concentration (C_i) as (Brooks and Farquhar, 1985):

$$J_G = \frac{(A + \nu R_d)(4C_i + 8\Gamma^*)}{C_i - \Gamma^*} \quad (2)$$

where Γ^* (μmol mol^{-1}) is the hypothetical CO_2 compensation point in the absence of R_d and ν is the proportion of dark respiration remaining during light (taken as 0.5 in this study; Villar et al., 1995). Standard temperature characteristics for Rubisco were used to determine Γ^* at different temperatures (Niinemets and Tenhunen, 1997). Because in these calculations default values for f_{PSII}, α, and ν were used, and in Equation 2 it is further assumed that the diffusion conductance for substomatal cavities (CO_2 concentration C_i) to chloroplasts (CO_2 concentration C_C) is large, both the estimates of electron transport calculated by Equations 1 and 2 are apparent rates. Nevertheless, previous studies demonstrate that estimations of photosynthetic electron transport rate are relatively insensitive to these assumptions for species having mesophytic leaves such as aspen (Laisk and Oja, 1998).

Isoprene Emission Rate and in Vivo DMADP Pool Size Measurements

Isoprene emission was measured with a proton transfer reaction mass spectrometer (PTR-MS; high-sensitivity version; Ionicon Analytik) with a response time of approximately 0.1 s and with a detection limit of approximately 10 pmol mol^{-1} (Lindinger et al., 1998; Hansel et al., 1999). The PTR-MS was calibrated with a standard gas (5.74 pmol mol^{-1} isoprene in N_2).

We used the recently developed in vivo method to estimate the DMADP pool size responsible for isoprene emission (Rasulov et al., 2009a). The method is based on integration of the amount of isoprene emitted during 150 to 200 s after leaf darkening (Rasulov et al., 2009a). The method assumes that dark release of isoprene emission is at the expense of DMADP formed during the light period. This assumption rests on the observations of rapid dark decay of ATP and NADPH needed for the synthesis of DMADP (Rasulov et al., 2009a; i.e. that no new chloroplastic DMADP is formed in the darkness or the contribution of dark-formed DMADP is small). Although leaf darkening also results in reductions in chloroplastic stroma pH from approximately 8 to 7 (Wu and Berkowitz, 1992; Nishio and Whitmarsh, 1993), IspS has a broad pH optimum between approximately 7 and 8.5 (Silver and Fall, 1991; Fall and Wildermuth, 1998; Wildermuth and Fall, 1998; Schnitzler et al., 2005) or even between 6.5 and 9 (Lehning et al., 1999). Thus, dark-light changes in pH are not expected to exert a rapid control over IspS activity.

In the previous measurements conducted with a relatively slow experimental setup, special effort was necessary to separate the gas-exchange system and plant responses. In the current experiments, with an overall gas-exchange system response time of approximately 3 s, the gas-exchange system contributed only a minor degree to the total postillumination isoprene signal (Fig. 9A); thus, the dark decay of isoprene emission was directly integrated.

At lower temperatures, isoprene emission approached zero at about 150 s after darkening. At higher temperatures, we also observed that a light-independent (B. Rasulov, Ü. Niinemets, and A. Laisk, unpublished data) isoprene emission process was initiated. Therefore, at higher temperatures, the baseline of the postillumination isoprene emission was adjusted to account

for the contribution of the light-independent component from zero at the time of darkening to the level of the longer term component at 150 to 200 s after darkening. Nevertheless, comparisons of the temperature responses obtained with the DMADP pools without this correction indicate that the contribution of the slower component within 150 to 200 s after darkening was small (on the order of 5%–10%), and the results were not qualitatively biased by the baseline correction introduced.

Experiments with Constant in Vivo DMADP Pool Size

In addition to the estimation of steady-state DMADP pools corresponding to each temperature (Fig. 9A), experiments with simultaneous changes of temperature upon leaf darkening were conducted (Fig. 9, B and C) to obtain temperature responses of leaf isoprene emission at a constant DMADP pool size. The baseline temperature of 33°C was used in these experiments, and we always waited at this temperature until the isoprene emissions reached a steady state before switching off the light for postillumination transients. In addition, in combined temperature and darkening transients, a delay of 6 s between the swap of the thermostats of the leaf chamber water jacket and switching off the light was applied to account for the somewhat slower temperature response of the system (Fig. 8). The idea was to synchronize the moment of darkening with the center of the leaf temperature change. We anticipated that about a constant DMADP pool was accumulated at 33°C, but its postillumination conversion to isoprene occurred at different temperatures. The results (Fig. 9) confirmed this, as the integral of postillumination isoprene release was very similar despite the fact that the postillumination process was carried out at different temperatures.

Estimation of the Rate Constant of IspS

In postillumination isoprene emission measurements, the rate of isoprene evolution decreases because the DMADP pool size is declining due to DMADP conversion into isoprene. At any time step of the postillumination curve, the isoprene reaction rate is recorded, while the pool of DMADP equals the integral of the rate from that moment until the cessation of isoprene emission. Such paired rates were estimated from the postillumination recordings and plotted against the DMADP pool still present at that moment. This resulted in IspS reaction versus DMADP pool size relationships corresponding to each temperature transient (Fig. 10). If the dark isoprene emission followed a first-order reaction kinetics under strongly substrate-limited conditions, as suggested by previous studies (Loreto et al., 2004; Rasulov et al., 2009a, 2009b), the relationship of DMADP pool size versus emission rate was linear. The primary condition for a first-order reaction is that the activation state of the enzyme stays constant during the postillumination isoprene release. In our study, all these responses were characterized by straight lines, as is expected from the exponential decay of a first-order reaction. Thus, the IspS reaction rate constant (s^{-1}) was calculated as the slope of the linear regression of isoprene emission versus DMADP pool size.

Data Analyses

The temperature dependencies of photosynthesis and isoprene emission characteristics were fitted by an Arrhenius-type response curve with a maximum:

$$y_i = \frac{e^{c-\Delta H_a/RT}}{1+e^{(\Delta ST-\Delta H_d)/RT}} \quad (3)$$

where y_i is the dependent variable, c is the scaling constant, ΔH_a (J mol^{-1}) is the activation energy, ΔH_d (J mol^{-1}) is the deactivation energy, ΔS (J mol^{-1} K^{-1}) is the entropy term, T (K) is the leaf temperature, and R (8.314 J mol^{-1} K^{-1}) is the gas constant. The optimum temperature of the given variable (T_{opt}) was determined as (Niinemets et al., 1999a):

$$T_{opt} = \frac{\Delta H_d}{\Delta S + R\ln\left(\frac{\Delta H_d}{\Delta H_a}-1\right)} \quad (4)$$

As ΔH_a, ΔH_d, and ΔS are fitted simultaneously in Equation 3, they are not necessarily independent for any given parameterization. To compare the activation energies for different processes, we also fitted the initial exponential part of the temperature response curve below the optimum by:

$$y_i = e^{c-\Delta H_a/RT} \quad (5)$$

In all cases, four to 10 replicate experiments were conducted, and average ± SD values were calculated. Whenever necessary, the means were compared by standard ANOVA, and the differences were considered significant at $P < 0.05$.

Received June 29, 2010; accepted September 12, 2010; published September 13, 2010.

LITERATURE CITED

Affek HP (2003) Isoprene emission from plants: physiological role and isotopic composition. PhD thesis. Weizmann Institute of Science, Rehovot, Israel

Brooks A, Farquhar GD (1985) Effects of temperature on the CO_2/O_2 specificity of ribulose-1,5-bisphosphate carboxylase/oxygenase and the rate of respiration in the light: estimates from gas-exchange measurements on spinach. Planta **165:** 397–406

Brüggemann N, Schnitzler JP (2002) Diurnal variation of dimethylallyl diphosphate concentrations in oak (*Quercus robur*) leaves. Physiol Plant **115:** 190–196

Centritto M, Calfapietra C, Alessio GA, Loreto F (2005) On the relationships between isoprene emission and light and dark respiration in hybrid poplars under free-air CO_2 enrichment. Geophys Res Abstr **7:** 10622

Chameides WL, Lindsay RW, Richardson J, Kiang CS (1988) The role of biogenic hydrocarbons in urban photochemical smog: Atlanta as a case study. Science **241:** 1473–1475

Cinege G, Louis S, Hänsch R, Schnitzler JP (2009) Regulation of isoprene synthase promoter by environmental and internal factors. Plant Mol Biol **69:** 593–604

Darbah JNT, Sharkey TD, Calfapietra C, Karnosky DF (2010) Differential response of aspen and birch trees to heat stress under elevated carbon dioxide. Environ Pollut **158:** 1008–1014

Fall R, Monson RK (1992) Isoprene emission rate and intercellular isoprene concentration as influenced by stomatal distribution and conductance. Plant Physiol **100:** 987–992

Fall R, Wildermuth MC (1998) Isoprene synthase: from biochemical mechanism to emission algorithm. J Geophys Res **103:** 25599–25609

Fehsenfeld F, Calvert J, Fall R, Goldan P, Guenther AB, Hewitt CN, Lamb B, Liu S, Trainer M, Westberg H, et al (1992) Emissions of volatile organic compounds from vegetation and the implications for atmospheric chemistry. Global Biogeochem Cycles **6:** 389–430

Fellermeier M, Raschke M, Sagner S, Wungsintaweekul J, Schuhr CA, Hecht S, Kis K, Radykewicz T, Adam P, Rohdich F, et al (2001) Studies on the nonmevalonate pathway of terpene biosynthesis: the role of 2C-methyl-D-erythritol 2,4-cyclodiphosphate in plants. Eur J Biochem **268:** 6302–6310

Fortunati A, Barta C, Brilli F, Centritto M, Zimmer I, Schnitzler JP, Loreto F (2008) Isoprene emission is not temperature-dependent during and after severe drought-stress: a physiological and biochemical analysis. Plant J **55:** 687–697

Guenther A, Karl T, Harley P, Wiedinmyer C, Palmer PI, Geron C (2006) Estimates of global terrestrial isoprene emissions using MEGAN (Model of Emissions of Gases and Aerosols from Nature). Atmos Chem Phys **6:** 3181–3210

Guenther AB, Zimmerman PR, Harley PC, Monson RK, Fall R (1993) Isoprene and monoterpene emission rate variability: model evaluations and sensitivity analyses. J Geophys Res **98:** 12609–12617

Hansel A, Jordan A, Warneke C, Holzinger R, Wisthaler A, Lindinger W (1999) Proton-transfer-reaction mass spectrometry (PTR-MS): on-line monitoring of volatile organic compounds at volume mixing ratios of a few pptv. Plasma Sources Sci Technol **8:** 332–336

Hanson DT, Sharkey TD (2001) Effect of growth conditions on isoprene emission and other thermotolerance-enhancing compounds. Plant Cell Environ **24:** 929–936

Harley P, Guenther A, Zimmerman P (1996) Effects of light, temperature and canopy position on net photosynthesis and isoprene emission from sweetgum (*Liquidambar styraciflua*) leaves. Tree Physiol **16:** 25–32

Harley P, Guenther A, Zimmerman P (1997) Environmental controls over isoprene emission in deciduous oak canopies. Tree Physiol **17:** 705–714

Hüve K, Bichele I, Rasulov B, Niinemets Ü (2010) When it is too hot for photosynthesis: heat-induced instability of photosynthesis in relation to respiratory burst, cell permeability changes and H_2O_2 formation. Plant Cell Environ (in press)

Kuzma J, Fall R (1993) Leaf isoprene emission rate is dependent on leaf development and the level of isoprene synthase. Plant Physiol **101:** 435–440

Laisk A, Oja V (1998) Dynamics of Leaf Photosynthesis: Rapid-Response Measurements and Their Interpretations. CSIRO Publishing, Canberra, Australia

Laisk A, Oja V, Rasulov B, Rämma H, Eichelmann H, Kasparova I, Pettai H, Padu E, Vapaavuori E (2002) A computer-operated routine of gas exchange and optical measurements to diagnose photosynthetic apparatus in leaves. Plant Cell Environ **25:** 923–943

Laisk A, Talts E, Oja V, Eichelmann H, Peterson RB (2010) Fast cyclic electron transport around photosystem I in leaves under far-red light: a proton-uncoupled pathway? Photosynth Res **103:** 79–95

Lehning A, Zimmer I, Steinbrecher R, Brüggemann N, Schnitzler JP (1999) Isoprene synthase activity and its relation to isoprene emission in *Quercus robur* L. leaves. Plant Cell Environ **22:** 495–504

Lichtenthaler HK (1998) The plants' 1-deoxy-D-xylulose-5-phosphate pathway for biosynthesis of isoprenoids. Lipid/Fett **100:** 128–138

Li-Cor (2001) Interfacing Custom Chambers to the LI-6400 Sensor Head. LI-6400 Portable Photosynthesis System: Application Note 3. Li-Cor, Lincoln, NE

Lindinger W, Hansel A, Jordan A (1998) Proton-transfer-reaction mass spectrometry (PTR-MS): on-line monitoring of volatile organic compounds at pptv levels. Chem Soc Rev **27:** 347–354

Loivamäki M, Louis S, Cinege G, Zimmer I, Fischbach RJ, Schnitzler JP (2007) Circadian rhythms of isoprene biosynthesis in grey poplar leaves. Plant Physiol **143:** 540–551

Loreto F, Centritto M, Barta C, Calfapietra C, Fares S, Monson RK (2007) The relationship between isoprene emission rate and dark respiration rate in white poplar (*Populus alba* L.) leaves. Plant Cell Environ **30:** 662–669

Loreto F, Pinelli P, Brancaleoni E, Ciccioli P (2004) ^{13}C labeling reveals chloroplastic and extrachloroplastic pools of dimethylallyl pyrophosphate and their contribution to isoprene formation. Plant Physiol **135:** 1903–1907

Loreto F, Sharkey TD (1990) A gas-exchange study of photosynthesis and isoprene emission in *Quercus rubra* L. Planta **182:** 523–531

Magel E, Mayrhofer S, Müller A, Zimmer I, Hampp R, Schnitzler JP (2006) Photosynthesis and substrate supply for isoprene biosynthesis in poplar leaves. Atmos Environ **40:** S138–S151

Mayrhofer S, Teuber M, Zimmer I, Louis S, Fischbach RJ, Schnitzler JP (2005) Diurnal and seasonal variation of isoprene biosynthesis-related genes in grey poplar leaves. Plant Physiol **139:** 474–484

Monson RK, Jaeger CH, Adams WW III, Driggers EM, Silver GM, Fall R (1992) Relationships among isoprene emission rate, photosynthesis, and isoprene synthase activity as influenced by temperature. Plant Physiol **98:** 1175–1180

Niinemets Ü, Arneth A, Kuhn U, Monson RK, Peñuelas J, Staudt M (2010a) The emission factor of volatile isoprenoids: stress, acclimation, and developmental responses. Biogeosciences **7:** 2203–2223

Niinemets Ü, Monson RK, Arneth A, Ciccioli P, Kesselmeier J, Kuhn U, Noe SM, Peñuelas J, Staudt M (2010b) The leaf-level emission factor of volatile isoprenoids: caveats, model algorithms, response shapes and scaling. Biogeosciences **7:** 1809–1832

Niinemets Ü, Oja V, Kull O (1999a) Shape of leaf photosynthetic electron transport versus temperature response curve is not constant along canopy light gradients in temperate deciduous trees. Plant Cell Environ **22:** 1497–1514

Niinemets Ü, Tenhunen JD (1997) A model separating leaf structural and physiological effects on carbon gain along light gradients for the shade-tolerant species *Acer saccharum*. Plant Cell Environ **20:** 845–866

Niinemets Ü, Tenhunen JD, Harley PC, Steinbrecher R (1999b) A model of isoprene emission based on energetic requirements for isoprene synthesis and leaf photosynthetic properties for *Liquidambar* and *Quercus*. Plant Cell Environ **22:** 1319–1336

Nishio JN, Whitmarsh J (1993) Dissipation of the proton electrochemical potential in intact chloroplasts. II. The pH gradient monitored by cytochrome *f* reduction kinetics. Plant Physiol **101:** 89–96

Nogués I, Brilli F, Loreto F (2006) Dimethylallyl diphosphate and geranyl diphosphate pools of plant species characterized by different isoprenoid emissions. Plant Physiol **141:** 721–730

Oja VM, Rasulov BH, Laisk AH (1988) An analysis of the temperature dependence of photosynthesis considering the kinetics of RuP_2 carboxylase and the pool of RuP_2 in intact leaves. Aust J Plant Physiol **15:** 737–748

Paulson SE, Flagan RC, Seinfeld JH (1992) Atmospheric photooxidation of isoprene. II. The ozone-isoprene reaction. Int J Chem Kinet **24:** 103–125

Pegoraro E, Rey A, Greenberg J, Harley P, Grace J, Malhi Y, Guenther A (2004) Effect of drought on isoprene emission rates from leaves of *Quercus virginiana* Mill. Atmos Environ **38:** 6149–6156

Rasulov B, Copolovici L, Laisk A, Niinemets Ü (2009a) Postillumination isoprene emission: in vivo measurements of dimethylallyldiphosphate pool size and isoprene synthase kinetics in aspen leaves. Plant Physiol **149:** 1609–1618

Rasulov B, Hüve K, Välbe M, Laisk A, Niinemets Ü (2009b) Evidence that light, carbon dioxide, and oxygen dependencies of leaf isoprene emission are driven by energy status in hybrid aspen. Plant Physiol **151:** 448–460

Rohdich F, Eisenreich W, Wungsintaweekul J, Hecht S, Schuhr CA, Bacher A (2001) Biosynthesis of terpenoids. 2*C*-methyl-D-erythritol 2,4-cyclodiphosphate synthase (IspF) from *Plasmodium falciparum*. Eur J Biochem **268:** 3190–3197

Rosenstiel TN, Potosnak MJ, Griffin KL, Fall R, Monson RK (2003) Increased CO_2 uncouples growth from isoprene emission in an agriforest ecosystem. Nature **421:** 256–259

Sanadze GN, Kalandadze AN (1966) Light and temperature curves of the evolution of C_5H_8. Russ J Plant Physiol **13:** 458–461

Sasaki K, Ohara K, Yazaki K (2005) Gene expression and characterization of isoprene synthase from *Populus alba*. FEBS Lett **579:** 2514–2518

Schnitzler JP, Arenz R, Steinbrecher R, Lehning A (1996) Characterization of an isoprene synthase from leaves of *Quercus petraea* (Mattuschka) Liebl. Bot Acta **109:** 216–221

Schnitzler JP, Zimmer I, Bachl A, Arend M, Fromm J, Fischbach RJ (2005) Biochemical properties of isoprene synthase in poplar (*Populus* x *canescens*). Planta **222:** 777–786

Schreiber U, Bilger W, Neubauer C (1994) Chlorophyll fluorescence as a nonintrusive indicator for rapid assessment of in vivo photosynthesis. *In* E-D Schulze, MM Caldwell, eds, Ecophysiology of Photosynthesis. Springer Verlag, Berlin, pp 49–70

Sharkey TD, Loreto F (1993) Water stress, temperature, and light effects on the capacity for isoprene emission and photosynthesis of kudzu leaves. Oecologia **95:** 328–333

Sharkey TD, Singsaas EL, Vanderveer PJ, Geron C (1996) Field measurements of isoprene emission from trees in response to temperature and light. Tree Physiol **16:** 649–654

Silver GM, Fall R (1991) Enzymatic synthesis of isoprene from dimethylallyl diphosphate in aspen leaf extracts. Plant Physiol **97:** 1588–1591

Singsaas EL, Laporte MM, Shi JZ, Monson RK, Bowling DR, Johnson K, Lerdau M, Jasentuliytana A, Sharkey TD (1999) Kinetics of leaf temperature fluctuation affect isoprene emission from red oak (*Quercus rubra*) leaves. Tree Physiol **19:** 917–924

Singsaas EL, Sharkey TD (1998) The regulation of isoprene emission responses to rapid leaf temperature fluctuations. Plant Cell Environ **21:** 1181–1188

Singsaas EL, Sharkey TD (2000) The effects of high temperature on isoprene synthesis in oak leaves. Plant Cell Environ **23:** 751–757

Stidham MA, Uribe EG, Williams GJ III (1982) The temperature dependence of photosynthesis in *Agropyron smithii* Rydb. II. Contribution from electron transport and photophosphorylation. Plant Physiol **69:** 929–934

Tingey DT, Evans R, Gumpertz M (1981) Effects of environmental conditions on isoprene emission from live oak. Planta **152:** 565–570

Vahala J, Keinänen M, Schützendübel A, Polle A, Kangasjärvi J (2003) Differential effects of elevated ozone on two hybrid aspen genotypes predisposed to chronic ozone fumigation: role of ethylene and salicylic acid. Plant Physiol **132:** 196–205

Villar R, Held AA, Merino J (1995) Dark leaf respiration in light and darkness of an evergreen and a deciduous plant species. Plant Physiol **107:** 421–427

von Caemmerer S, Farquhar GD (1981) Some relationships between the

biochemistry of photosynthesis and the gas exchange of leaves. Planta **153:** 376–387

Weiss I, Mizrahi Y, Raveh E (2009) Chamber response time: a neglected issue in gas exchange measurements. Photosynthetica **47:** 121–124

Wiberley AE, Donohue AR, Meier ME, Westphal MM, Sharkey TD (2008) Regulation of isoprene emission in *Populus trichocarpa* leaves subjected to changing growth temperature. Plant Cell Environ **31:** 258–267

Wiberley AE, Donohue AR, Westphal MM, Sharkey TD (2009) Regulation of isoprene emission from poplar leaves throughout a day. Plant Cell Environ **32:** 939–947

Wiberley AE, Linskey AR, Falbel TG, Sharkey TD (2005) Development of the capacity for isoprene emission in kudzu. Plant Cell Environ **28:** 898–905

Wildermuth MC, Fall R (1996) Light-dependent isoprene emission: characterization of a thylakoid-bound isoprene synthase in *Salix discolor* chloroplasts. Plant Physiol **112:** 171–182

Wildermuth MC, Fall R (1998) Biochemical characterization of stromal and thylakoid-bound isoforms of isoprene synthase in willow leaves. Plant Physiol **116:** 1111–1123

Wilkinson MJ, Monson RK, Trahan N, Lee S, Brown E, Jackson RB, Polley HW, Fay PA, Fall R (2009) Leaf isoprene emission rate as a function of atmospheric CO_2 concentration. Glob Change Biol **15:** 1189–1200

Wolfertz M, Sharkey TD, Boland W, Kuehnemann F, Yeh S, Weise SE (2003) Biochemical regulation of isoprene emission. Plant Cell Environ **26:** 1357–1364

Wu W, Berkowitz GA (1992) Stromal pH and photosynthesis are affected by electroneutral K^+ and H^+ exchange through chloroplast envelope ion channels. Plant Physiol **98:** 666–672

Zhang R, Cruz JA, Kramer DM, Magallanes-Lundback ME, Dellapenna D, Sharkey TD (2009) Moderate heat stress reduces the pH component of the transthylakoid proton motive force in light-adapted, intact tobacco leaves. Plant Cell Environ **32:** 1538–1547

Zhang R, Sharkey TD (2009) Photosynthetic electron transport and proton flux under moderate heat stress. Photosynth Res **100:** 29–43

Zimmer W, Brüggemann N, Emeis S, Giersch C, Lehning A, Steinbrecher R, Schnitzler JP (2000) Process-based modelling of isoprene emission by oak leaves. Plant Cell Environ **23:** 585–595